

# The water-absorption region of ventral skin of several semiterrestrial and aquatic anuran amphibians identified by aquaporins

Yuji Ogushi, Azumi Tsuzuki, Megumi Sato, Hiroshi Mochida, Reiko Okada, Masakazu Suzuki, Stanley D. Hillyard and Shigeyasu Tanaka

*Am J Physiol Regul Integr Comp Physiol* 299:R1150-R1162, 2010. First published 1 September 2010; doi:10.1152/ajpregu.00320.2010

---

## You might find this additional info useful...

---

This article cites 35 articles, 16 of which can be accessed free at:

<http://ajpregu.physiology.org/content/299/5/R1150.full.html#ref-list-1>

Updated information and services including high resolution figures, can be found at:

<http://ajpregu.physiology.org/content/299/5/R1150.full.html>

Additional material and information about *American Journal of Physiology - Regulatory, Integrative and Comparative Physiology* can be found at:

<http://www.the-aps.org/publications/ajpregu>

---

This information is current as of April 1, 2011.

# The water-absorption region of ventral skin of several semiterrestrial and aquatic anuran amphibians identified by aquaporins

Yuji Ogushi,<sup>1\*</sup> Azumi Tsuzuki,<sup>2\*</sup> Megumi Sato,<sup>1</sup> Hiroshi Mochida,<sup>3</sup> Reiko Okada,<sup>1</sup> Masakazu Suzuki,<sup>2</sup> Stanley D. Hillyard,<sup>4</sup> and Shigeyasu Tanaka<sup>1,2</sup>

<sup>1</sup>Integrated Bioscience Section, Graduate School of Science and Technology, Shizuoka University, Shizuoka, Japan;

<sup>2</sup>Department of Biology, Faculty of Science, Shizuoka University, Shizuoka, Japan; <sup>3</sup>Protein Purify Company, Gunma, Japan; and <sup>4</sup>School of Dental Medicine, University of Nevada, Las Vegas, Nevada

Submitted 13 May 2010; accepted in final form 28 August 2010

**Ogushi Y, Tsuzuki A, Sato M, Mochida H, Okada R, Suzuki M, Hillyard SD, Tanaka S.** The water-absorption region of ventral skin of several semiterrestrial and aquatic anuran amphibians identified by aquaporins. *Am J Physiol Regul Integr Comp Physiol* 299: R1150–R1162, 2010. First published September 1, 2010; doi:10.1152/ajpregu.00320.2010.—Regions of specialization for water absorption across the skin of Bufonid and Ranid anurans were identified by immunohistochemistry and Western blot analysis, using antibodies raised against arginine vasotocin (AVT)-stimulated aquaporins (AQPs) that are specific to absorbing regions of *Hyla japonica*. In *Bufo marinus*, labeling for *Hyla* urinary bladder-type AQP (AQP-h2), which is also localized in the urinary bladder, occurred in the ventral surface of the hindlimb, pelvic, and pectoral regions. AQP-h2 was not detected in any skin regions of *Rana catesbeiana*, *Rana japonica*, or *Rana nigromaculata*. *Hyla* ventral skin-type AQP (AQP-h3), which is found in the ventral skin but not the bladder of *H. japonica*, was localized in the hindlimb, pelvic, and pectoral skins of *Bufo marinus*, in addition to AQP-h2. AQP-h3 was also localized in ventral skin of the hindlimb of all three *Rana* species and also in the pelvic region of *R. catesbeiana*. Messenger RNA for AQP-x3, a homolog of AQP-h3, could be identified by RT-PCR from the hindlimb, pectoral, and pelvic regions of the ventral skin of *Xenopus laevis*, although AVT had no effect on water permeability. In contrast,  $10^{-8}$  M AVT-stimulated water permeability and translocation of AQP-h2 and AQP-h3 into the apical membrane of epithelial cells in regions of the skin of species where they had been localized by immunohistochemistry and Western blot analysis. Finally, water permeability of the hindlimb skin of *B. marinus* and all the *Rana* species was stimulated by hydriins 1 and 2 to a similar level as seen for AVT. The present data demonstrate species differences in the occurrence, distribution, and regulation of AQPs in regions of skin specialized for rapid water absorption that can be associated with habitat and also phylogeny.

hindlimb skin; arginine vasotocin; immunohistochemistry; water permeability; frogs

MANY ADULT ANURAN AMPHIBIANS do not drink through their mouth. Rather, they absorb water across their skin and form dilute urine that is stored in their urinary bladder and can be reabsorbed when foraging away from a hydration source (4, 5). Hillman et al. (14) refer to this water balance strategy as semiterrestrial to distinguish it from terrestrial species that are completely independent of water. The semiterrestrial classification applies to tree frogs in the family Hylidae and toads in

the family Bufonidae that have been traditionally classified as arboreal and terrestrial, respectively, in that both have large urinary bladder capacity and specializations for rapidly rehydrating when water is available. Specifically, they utilize an area of skin in the posteroventral region of the body that is specialized for rapid water absorption from shallow water sources or moist substrates. This region, termed the pelvic patch or seat patch, extends laterally to the ventral surface of the hindlimbs and shows a pattern of elevations and grooves termed verrucae hydrophilicae (14). The seat patch is also an area where capillaries form intimate contact with the basement membrane that underlies the epithelium. These structures are less well developed or absent in anuran species such as frogs in the family Ranidae that Hillman et al. (14) refer to as semiaquatic, because they are more dependent on a permanent source of water but may forage considerable distances in moist (mesic) habitats (10).

Literature values in vivo and with isolated skin indicate the semiaquatic Ranid species show a smaller response to arginine vasotocin (AVT) relative to the more xeric Hylid and Bufonid species (4) that have specialized regions for cutaneous water absorption. The mechanism for baseline and AVT-stimulated water permeability is controlled by aquaporins (AQPs), a class of integral membrane proteins that form selective water channels (pores) in the plasma membranes of various cells in virtually all organisms (1, 17, 23, 30). AVT stimulation results in the fusion of subapical vesicles containing the AQPs, with the apical membrane of epithelial tissues specialized for water absorption and reabsorption.

Recently, our group used RT-PCR to identify two forms of AVT-stimulated AQP in epithelial tissues of the skin of the tree frog, *Hyla japonica*: AQP-h2 was found in the urinary bladder, as well as the pelvic skin region (13, 20, 31). AQP-h2-like AQPs are also localized in the urinary bladder of *Rana* and *Bufo* species (20, 27) and have been referred to as the “urinary bladder-type” amphibian AQP (20). The second isoform, AQP-h3, was characterized from the ventral skin but not the urinary bladder of *H. japonica* (31). AQP-h3-like AQPs have similarly been characterized in ventral skin but not the bladder of *Hyla*, *Bufo*, and *Rana* species and have been termed the “ventral skin-type” AQP (20). This tissue distribution of AQP-h2 and AQP-h3 isoforms is provided in Table 1.

A subfamily of AQPs, termed aquaglyceroporins occurs in the basolateral membranes of water-transporting epithelia (1, 17) and is permeated by glycerol and urea in addition to water. In amphibians, these include AQP-h3BL, homologue of mammalian AQP3, in *H. japonica* (2), and AQP HC-3 in *H. chrysoscelis* (37). Such channels facilitate the movement of

\* Y. Ogushi and A. Tsuzuki contributed equally to this work.

Address for reprint requests and other correspondence: S. Tanaka, Integrated Bioscience Section, Graduate School of Science and Technology, Shizuoka Univ., Ohya836, Suruga-ku, Shizuoka 422-8529, Japan (e-mail: sbstana@ipc.shizuoka.ac.jp).

Table 1. Phylogenetic distribution of aquaporins in the ventral pelvic skins of anuran species living in different habitats

Habitat	Species	Pelvic Skin		Urinary Bladder
		AQP-h2-Like Protein (Urinary Bladder-Type)	AQP-h3-Like cDNA (Ventral Pelvic-Type)	AQP-h2-Like Protein (Urinary Bladder-Type)
Arboreal	<i>Hyla japonica</i>	+	+	+
Terrestrial	<i>Bufo japonica</i>	+	+	+
Semiaquatic	<i>Rana catesbeiana</i>	–	+	+
Semiaquatic	<i>Rana nigromaculata</i>	–	+	+
Semiaquatic	<i>Rana japonica</i>	–	+	+*
Aquatic	<i>Xenopus laevis</i>	–	+	+

+, presence; –, absence. \*Unpublished data

water out of the cells into the vasculature, but the rate-limiting step is apical entry that is regulated by AVT and possibly other factors. The first objective of this study was to critically examine the relationship between AQP distribution in the apical membranes and AVT stimulation of water permeability in three zones (hindlimb, pelvic, and pectoral) of the ventral skin of toads (*Bufo marinus*) and frogs (*Rana catesbeiana*, *Rana japonica*, and *Rana nigromaculata*). This allowed a more detailed examination of the hypothesis put forth by Bentley and Main (4) that water permeability and its regulation by AVT differ among anuran species depending upon their habitat, and we suggest that phylogenetic factors should also be considered.

More recently, we have found AQP-x3 mRNA, that is homologous to AQP-h3, is expressed in the pelvic skin of the aquatic species, *Xenopus laevis*, but the mRNA is not translated to AQP-x3 protein (20). Given the different patterns of regional specialization seen in terrestrial, arboreal, and semiaquatic species, the second objective of this study was to examine the expression of AQP-x3 mRNA in the skin of the hindlimb, pelvic, pectoral, and dorsal regions.

In addition to AVT, hydrins are intermediate peptides derived from a proasotocin-neurophysin precursor. Like AVT, hydrins stimulate osmotic water movement across the skin and bladder but are devoid of antidiuretic activity in the kidney (19, 24). Hydrins are only present in anuran amphibians, and we found that hydrin 1 and hydrin 2, as well as AVT, have stimulatory effects on the water permeability across the pelvic skin in *H. japonica* (21). The third objective of this study was to extend these observations and compare them with the response of the Ranid and Bufonid species to AVT.

## MATERIALS AND METHODS

**Animals.** Sexually mature *Rana japonica*, *Rana nigromaculata*, *Rana catesbeiana*, and *X. laevis* of both sexes were purchased from a commercial dealer (Ouchi, Saitama, Japan). Sexually mature *Bufo marinus* were collected in the field on Ishigaki Island, Okinawa. While *X. laevis* was kept in water, the other frogs and toads were in containers with a small amount of water for about 2 wk at 25–27°C before use. They were fed European crickets or trout pellets twice a week. All the experiments were performed from June to September. Skin for experimental treatments was removed under anesthesia (MS222; Nacalai Tesque, Kyoto, Japan). All animal experiments were carried out in compliance with the Guide for Care and Use of Laboratory Animals of Shizuoka University and approved by its ethics committee.

**Immunohistochemistry.** Ventral skin from the pectoral, pelvic, and hindlimb regions of *B. marinus* and the three *Rana* species was fixed overnight in periodate-lysine-paraformaldehyde (PLP) fixative, dehydrated, and embedded in Paraplast. Four-micrometer sections were cut and mounted on gelatin-coated slides. The deparaffinized sections

were rinsed with PBS. For *Rana* species, the sections were incubated with rabbit anti-AQP-h3 (ST-141; 1:10,000, 31) and then reacted with Alexa Fluor 488-labeled donkey anti-rabbit IgG (1:200; Molecular Probes, Eugene, OR) containing 4',6-diamidino-2-phenylindole (DAPI) for nuclear counterstaining. To investigate the specificity of the immunoreaction, we performed an absorption test by preincubating anti-AQP-h3 antibody with the antigen peptide (10 µg/ml). For *B. marinus* skin, double-immunofluorescence labeling was carried out according to Hasegawa et al. (13). In brief, sections were also incubated with guinea pig anti-*Hyla* AQP-h2 serum (ST-140; 1:5,000, 13) followed by indocarbocyanine (Cy3)-labeled goat anti-guinea pig IgG (1:200; Jackson Immunoresearch, West Grove, PA). As with AQP-h3, specificity was performed by preincubating anti-AQP-h3 antibody with the antigen peptide (10 µg/ml). Specimens were examined with an Olympus BX61 microscope equipped with a BX-epifluorescence attachment (Olympus Optical, Tokyo, Japan).

**Western blot analysis.** Pieces of ventral skin from pectoral, pelvic, and hindlimb regions of *B. marinus* and the *Rana* species were homogenized in cell lysis buffer (50 mM Tris-HCl, pH 8.0, 0.15 M NaCl, 1% Triton X-100, 0.1 mg/ml PMSF, 1 mg/ml aprotinin) and centrifuged at 16,000 g in a microcentrifuge for 10 min to remove insoluble materials. The protein (10 µg) was denatured at 70°C for 10 min in denaturation buffer comprising 3% SDS, 70 mM Tris-HCl, pH 6.8, 11.2% glycerol, 5% 2-mercaptoethanol, and 0.01% bromophenol blue, subjected to electrophoresis on a 12% polyacrylamide gel, and then transferred to an Immobilon-P membrane (Millipore, Tokyo, Japan). The proteins on the membrane were reacted sequentially with rabbit anti-AQP-h3 serum (ST-141) or guinea pig anti-AQP-h2 serum (ST-140) followed by biotinylated goat anti-rabbit IgG (Jackson Immunoresearch, West Grove, PA) or biotinylated goat anti-guinea pig IgG (Jackson Immunoresearch). Immunopositive bands were visualized as reaction products of streptavidin-conjugated horseradish peroxidase (DAKO Japan, Kyoto, Japan) using an ECL Western Blot Detection kit (Amersham Pharmacia Biotech, Buckinghamshire, UK). To check the specificity of the immunoreaction, we performed an absorption test by preincubating the antibodies with the antigen peptide (10 µg/ml).

**RT-PCR of *Xenopus* ventral skin.** RT-PCR for AQP-x3 was conducted for ventral pectoral, pelvic, hindlimb, and dorsal skin. TRIzol reagent (Invitrogen, Tokyo, Japan) was used to prepare total RNA from parts of ventral skin. Total RNA (20 µg) was first treated with DNase I (4 U; Takara, Kyoto, Japan), following which a 10-µg aliquot of the total RNA product was reverse transcribed with M-MLV-reverse transcriptase (Invitrogen) at 37°C for 1 h and then inactivated at 70°C for 30 min. The RT-PCR analysis was performed according to the method of Ogushi et al. (22), using the following primers: primer 1 (sense) GTGACACTAGCATTCCTCTT (224–244 b) and primer 2 (antisense) GCAGCCAGTGAAGTAAATCC (537–557 b). *Xenopus* β-actin (accession no.: BC082343) primers were used as a control for the RT-PCR, β-actin sense primer was 5'-ACGTGACCTGACAGACTACC-3' (579–598 bp) and the antisense, was CAGTATTGGCATAGAGGTCC-3' (906–917 bp). The RT-PCR products

were analyzed on a 2% agarose gel containing ethidium bromide (0.5  $\mu\text{g/ml}$ ).

The PCR products were purified following gel electrophoresis and sequenced using DNA sequencer [model Lic-4200L(S); Aloka, Tokyo, Japan].

**Experimental protocol for water permeability.** Water permeability was measured across isolated skin from the pectoral, pelvic, and hindlimb regions of *B. marinus* and the *Rana* species. Animals were immersed in water for 30 min before being killed to ensure a fully hydrated state for control observations (21). The isolated skin was washed with Ringer solution and then mounted between two chambers connected by an opening having a diameter of 1 cm. The chamber on the serosal side of the skin was filled with a Ringer solution (in millimoles per liter): 113 NaCl, 1.9 KCl, 1.1 CaCl<sub>2</sub>, 0.06 NaH<sub>2</sub>PO<sub>4</sub>, and 1.4 NaHCO<sub>3</sub> having an osmolarity of 220 mOsm/l, while the mucosal chamber was filled with water. Water movement from the mucosal to the serosal side of the skin was measured directly using a 0.1-ml pipette attached the serosal chamber of the apparatus (21). Water movement recorded over a 30-min period with the Ringer solution in the mucosal chamber followed by a 30-min period with Ringer solution containing 10<sup>-8</sup> M AVT. After incubation, the skins were examined by immunofluorescence microscopy, as described above, to evaluate incorporation of AQP-h3 and AQP-h2 into the apical membrane of the first reacting cell (FRC) layer that is joined by tight junction to form a continuous barrier between the outside and inside of the body (6, 7, 11, 13, 35).

In a second set of experiments the effect of AVT on water permeability across the hindlimb skin only was compared with that to the same concentration (10<sup>-8</sup> M) of hydrin 1 and hydrin 2. To verify that AVT-stimulated water flux was mediated by AQPs, the effect of HgCl<sub>2</sub> on water transport across the hindlimb skins was measured. Skins were pretreated with 10<sup>-8</sup> M AVT for 10 min to increase the number of AQPs inserted in the apical plasma membrane followed by treatment of the skins with 0.3 mM HgCl<sub>2</sub> solution for 10 min. Water movement with continued AVT treatment was measured for an additional 30 min. Results from 5 or 6 individuals were expressed as means  $\pm$  SE.

**Statistical analysis.** The data were compared by the Steel-Dwass's test using PASW Statistics 18 software (SPSS, Chicago, IL). Statistical significance was considered as  $P < 0.05$ .

## RESULTS

**Characterization of aquaporins in three regions of ventral skin.** Ventral skin from *R. japonica* and *R. nigromaculata* (Figs. 1A and 2A), showed immunoreactive staining for AQP-h3 in the principal cells of the hindlimb region (Figs. 1B and 2B). Nomarski images of the same sections (Figs. 1C and 2C) showed that intense labeling was predominantly found in the basolateral membrane of cells in the FRC. This positive reaction was abolished by preincubation with the antigen peptide (Figs. 1, D and E and 2, D and E). Positive labeling was not visible in the pelvic (Figs. 1, F and G and 2, F and G) or pectoral (Figs. 1, H and I and 2, H and I) regions. Positive bands were seen in Western blots at  $\sim$ 29 kDa with smeary bands of higher molecular mass in the hindlimb skin (Fig. 1, J, a, lane I and Fig. 2, J, a, lane I). A positive band was not detected in skin from the pelvic (Fig. 1, J, a, lane II and Fig. 2, J, a, lane II) or pectoral (Fig. 1, J, a, lane III and Fig. 2, J, a, lane III) regions. Positive bands were not seen when the antibody was preincubated with the antigen peptide (Figs. 1, J, b and 2, J, b).

In ventral skin of *R. catesbeiana* (Fig. 3A), the greatest number of labeled cells and the intensity of labeling with AQP-h3 antibody were similarly observed in principal cells of

the hindlimb (Fig. 3, A–C), and the positive reaction was abolished by preincubation with the respective antigen peptide (Fig. 3, D and E). Unlike *R. japonica* or *R. nigromaculata*, a small number of principal cells in the pelvic skin were moderately labeled by the AQP-h3 antibody (Fig. 3, A, F, and G). For both hindlimb and pelvic skin, the label was localized in the basolateral plasma membrane. However, in the pectoral region, a positive reaction was observed as a dot spot only in the cytoplasm of a few principal cells in the FRC layer (Figs. 3, A, H, and I). When the extracts of the hindlimb, pelvic, and pectoral skins from *R. catesbeiana* were subjected to Western blot analysis, positive bands were found at  $\sim$ 29 kDa (Fig. 3, J, a), although the intensity of the band decreased gradually from the hindlimb skin to the pectoral skin (Fig. 3, J, a, lanes I–III). These positive bands disappeared when antiserum was preincubated with the antigen (Fig. 3, J, b).

Ventral skin from *B. marinus* (Fig. 4A) showed immunopositive labeling for AQP-h3 and AQP-h2 in principal cells of the hindlimb (Fig. 4, B and D), pelvic (Fig. 4, F and H), and pectoral (Fig. 4, J and L) regions. The positive reactions in each region were abolished when the antibodies were preabsorbed with the respective peptides (Fig. 4, C, E, G, I, K, and M). Labeling was predominantly observed in the cytoplasm just beneath the apical membrane; however, the number of the principal cells labeled with anti-AQP-h3 and AQP-h2 varied among toads. In some toads, the number of cells immunopositive for AQP-h3 and AQP-h2 was high in all regions, while in other toads the greatest number of cells and intensity of labeling were observed in the hindlimb and pelvic skins, but less labeling was seen in the pectoral skin. Fig. 4 (B–M) illustrates a representative experiment in which the number of principal cells labeled for AQP-h3 and AQP-h2 decreased from the hindlimb skin to the pectoral skin. Western blot analysis revealed a major positive band for AQP-h3 at  $\sim$ 29 kDa in the hindlimb, pelvic, and pectoral skin (Fig. 4, N, a, lanes I, II, and III). A smeary band at higher molecular mass was frequently observed as well. A major band for AQP-h2 protein with a smeary band at higher molecular mass was similarly observed at  $\sim$ 29 kDa in the hindlimb, pelvic, and pectoral regions (Fig. 4, O, a, lanes I–III). The intensity of both the bands decreased from the hindlimb to the pectoral skin. These positive bands disappeared when the antisera were preabsorbed with the respective antigen peptides (Fig. 4, N, b and O, b).

In *X. laevis*, we examined AQP-x3 mRNA levels in the same three regions of the ventral skin (Fig. 5A). Using RT-PCR, we were able to detect AQP-x3 mRNA expression in skin from the pectoral, pelvic, and hindlimb regions but not in dorsal skin (Fig. 5B). The cDNA fragments of AQP-x3 amplified by the RT-PCR showed a range of 223 to 555 bp in the full-length sequence (data not shown), indicating that the RNA amplified by the RT-PCR is a product of the AQP-x3.

**Water permeability and dynamic movement of AQP-h3 and AQP-h2 immunopositive substances after stimulation of AVT and hydrins.** Water permeability across the skin from the hindlimb, but not the pelvic or pectoral regions, of *R. japonica* and *R. nigromaculata* was significantly stimulated by AVT (Fig. 6, A and B). AVT stimulation of water permeability of skin from *R. catesbeiana* increased in order of the pectoral, pelvic, and hindlimb regions, but it was significantly greater in the hindlimb region, reaching levels similar to those of *R. japonica* and *R. nigromaculata* (Fig. 6C). AVT stimulation of

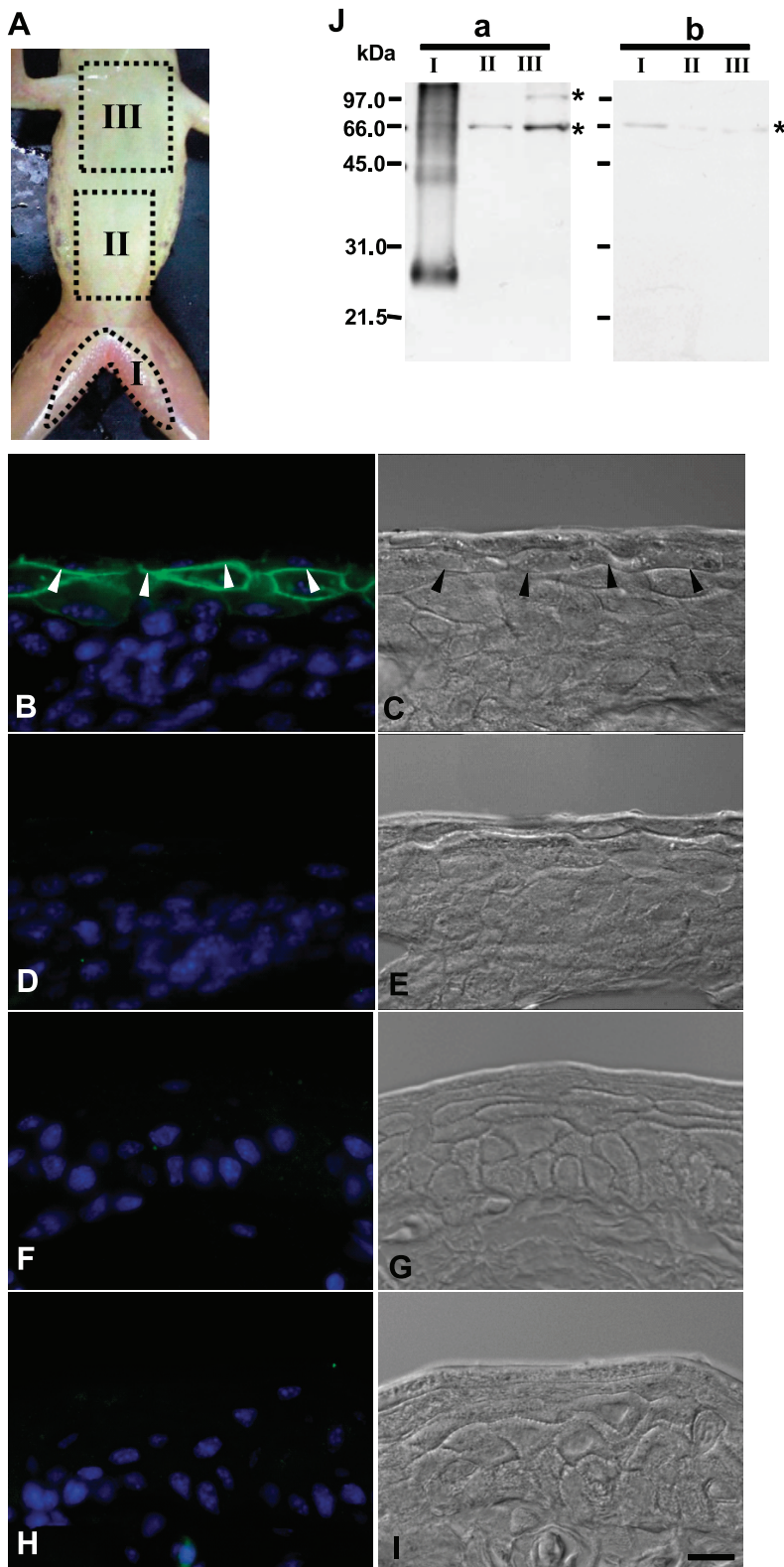


Fig. 1. The ventral skin of *Rana japonica* was divided into three regions: hindlimb (I), pelvic (II), and pectoral skins (III). A: pelvic skin-type aquaporin (AQP; green) was expressed in the hindlimb skin (B), but not in the pelvic (F) and pectoral (H) skins. The positive label was visible in the basolateral, apical, and cytoplasm in the principal cells in the first reacting cell layer. D: in the absorption test, the immunopositive substances disappeared in the principal cells. The corresponding Nomarski images (C, E, G, and I) refer to B, D, F and H, respectively. Arrowheads indicate the positive-labeled basolateral plasma membrane in the first reacting cell layer. Nuclei are counterstained with 4',6-diamidino-2-phenylindole (DAPI) (blue). Scale bar = 10  $\mu$ m. Western blot analysis (J, a) detected a major band at  $\sim$ 29 kDa in the hindlimb skin (lane I), but no band was seen in the extract of pelvic (lane II) and pectoral (lane III) skins. In the absorption test (J, b), the immunopositive band in the hindlimb skin disappeared (lane I). Asterisks denote nonspecific bands.

water permeability across the ventral skin of *B. marinus* was variable depending upon individuals and regions of ventral skin but was consistently above the control values (Fig. 6D). In three of the six toads, the response to AVT was greatest in the hindlimb skin and declined in the pelvic and pectoral skin,

while in the other three, the response was greatest in the pelvic skin.

Following AVT treatment, hindlimb skin of *R. japonica* and *R. nigromaculata*, showed positive immunostaining for anti-AQP-h3 in the apical plasma membrane in the principal cells of

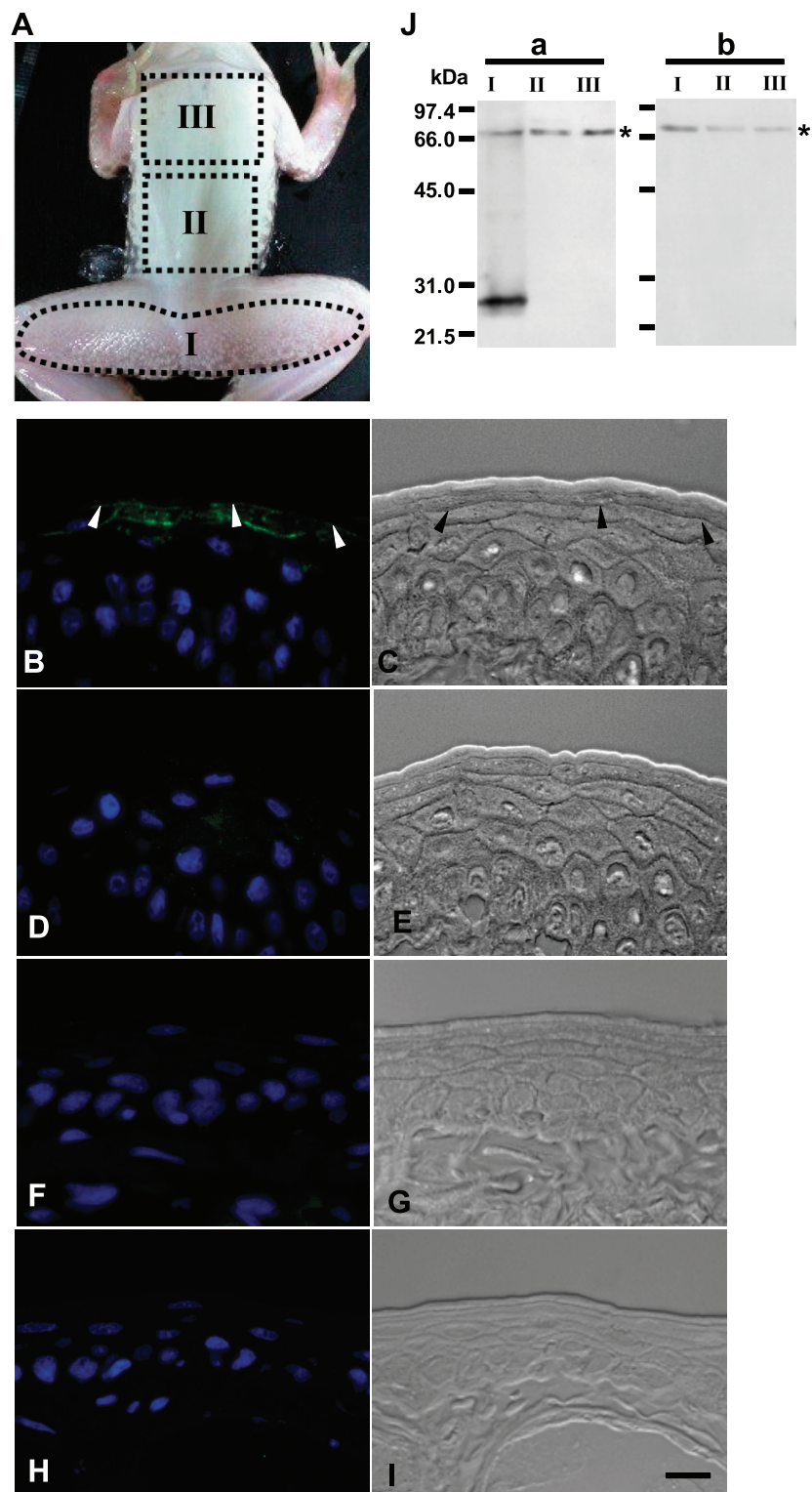


Fig. 2. The ventral skin of *Rana nigromaculata* was divided into three regions: hindlimb (I), pelvic (II), and pectoral skins (III) A: pelvic type-AQP (green) is expressed in the hindlimb (B), but not in the pelvic (F) and pectoral (H) skins. The positive label was visible in the basolateral plasma membrane of principal cells (arrowheads) in the first reacting cell layer. D: when the antibody was preabsorbed with the peptide, the immunopositive substances disappeared in the principal cells. The corresponding Nomarski images (C, E, G, and I) refer to B, D, F, and H, respectively. Nuclei were counterstained with DAPI (blue). Scale bar = 10  $\mu$ m. Western blot analysis (J, a) detected a major band at  $\sim$ 29 kDa only in the hindlimb skin (lane I), but no band was seen without non-specific band in the pelvic (lane II) and pectoral (lane III) skins. In the absorption test (J, b), the immunopositive band in the hindlimb skin disappeared (lane I). Asterisks denote nonspecific bands.

FRC layer (Fig. 7, A and C). As before, Nomarski images were shown for each slide to identify the site of immunostaining (Fig. 7, B and D). For *R. catesbeiana*, the translocation of immunoreactive AQP-h3 protein to the apical plasma membrane of principal cells in the FRC layer was also greater in the hindlimb region and decreased in pelvic and pectoral regions that showed a lower stimulation of water permeability by AVT

(Figs. 6C and 8). In *B. marinus*, the translocation of AQP-h3- and AQP-h2-positive proteins to the apical plasma membrane of principal cells in the FRC layer of the hindlimb, pelvic, and pectoral regions occurred in proportion to the stimulation of water permeability following AVT treatment (Fig. 9). Water permeability across *X. laevis* skin was not stimulated by AVT in any of the three regions (data not shown).

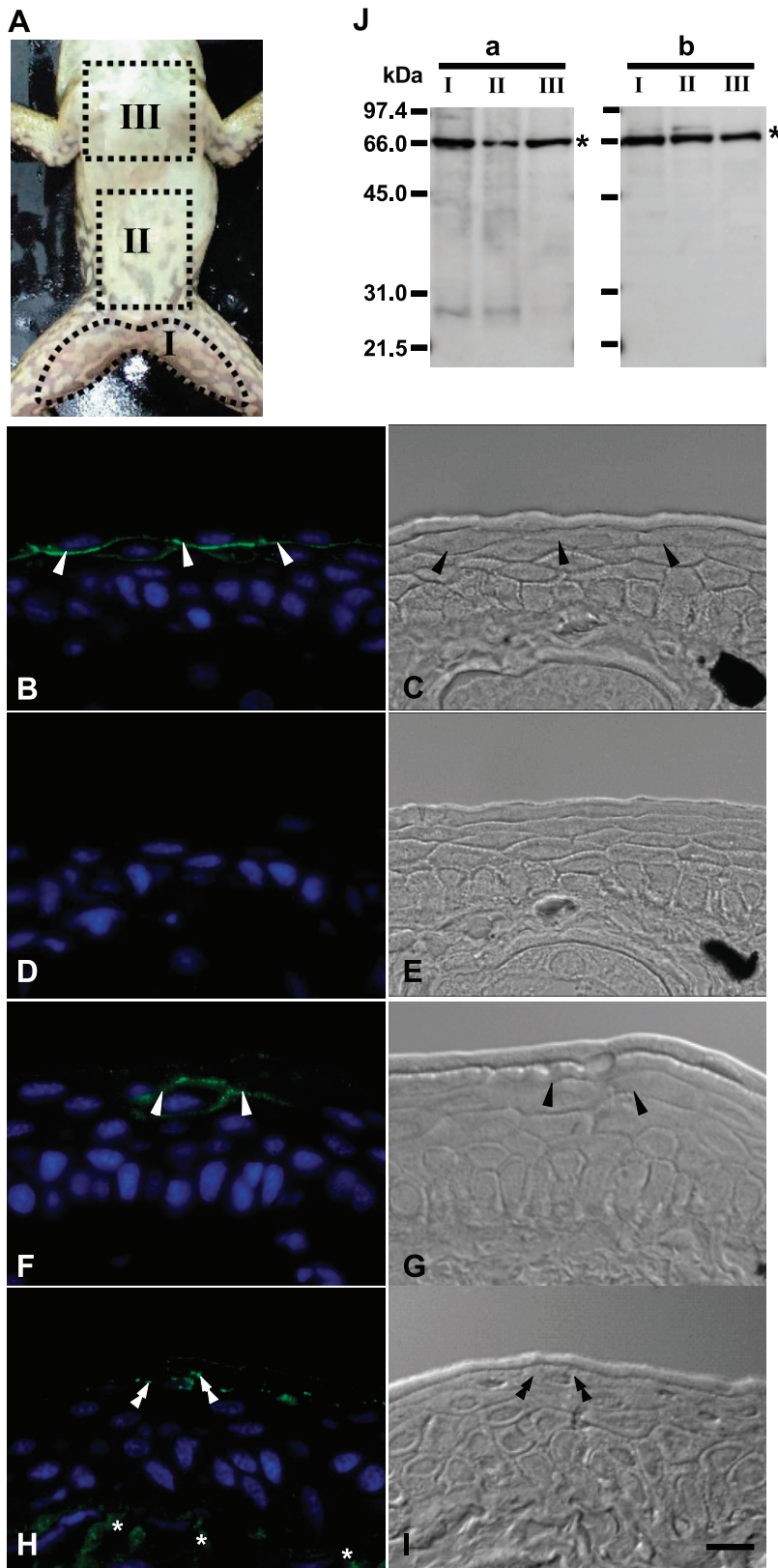


Fig. 3. The ventral skin of *Rana catesbeiana* was divided into three regions: hindlimb (I), pelvic (II), and pectoral skins (III) A: pelvic skin-type AQP protein (green) was expressed in the hindlimb (B), pelvic (F), and pectoral (H) skins. The intensity of labeling in the basolateral plasma membrane (arrowheads) of principal cells in the first reacting cell layer decreased from the hindlimb to the pectoral skin (B, F–I). The positive labels (double arrowheads) were visible in the cytoplasm of principal cells in the pectoral skin (H). In the absorption test, the immunopositive substances disappeared in the principal cells (D). The corresponding Nomarski images (C, E, G, and I) refer to B, D, F, and H, respectively. Nuclei are counterstained with DAPI (blue). Asterisks indicate nonspecific labeling. Scale bar = 10  $\mu$ m. Western blot analysis (J, a) detected a major band at ~29 kDa and a smeary band with higher molecular masses in the hindlimb skin (lane I). Weak bands were also visible at the identical position in the pelvic skin (lane II), but, unlike the immunohistochemical staining, AQP-h3 was not identified in the pectoral skin (lane III). In the absorption test (J, b), the immunopositive band disappeared in these regions (lanes I–III). Asterisks indicate nonspecific bands.

AVT, hydrin 1, and hydrin 2, significantly increased the water permeability of hindlimb skin ( $P < 0.05$ ) in *R. japonica* > *R. nigromaculata* > *R. catesbeiana* > *B. marinus* (Fig. 10). There were no significant differences among the hormone re-

sponses within a given species (Fig. 10). The increased rates of water flux by AVT and its related peptides relative to the control values were 30–38 times in *R. japonica* (Fig. 10A), ~15 times in *R. nigromaculata* (Fig. 10B), 8–12 times in *R. catesbeiana* (Fig.

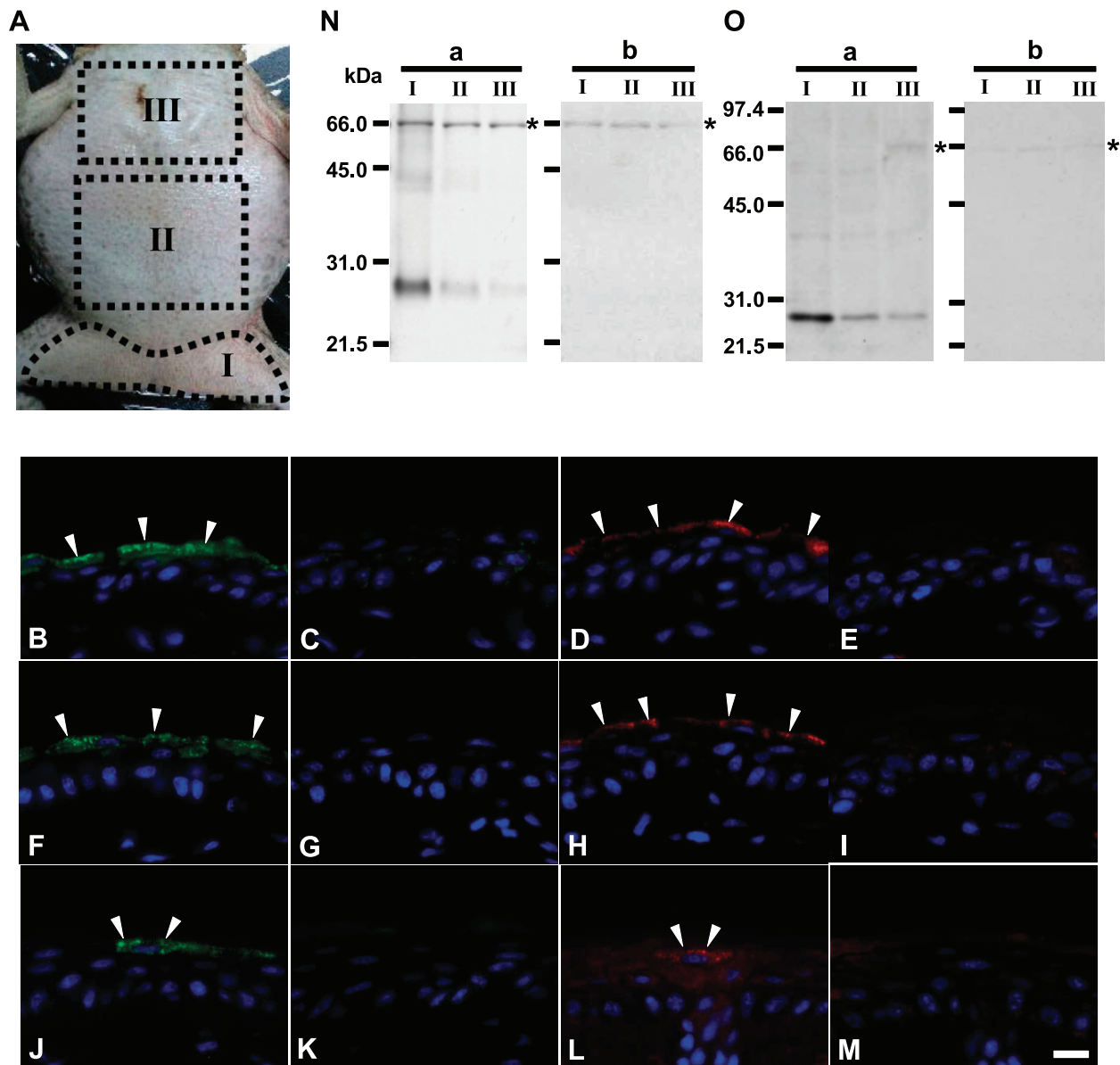


Fig. 4. The ventral skin of *Bufo marinus* (A) was divided into three regions: hindlimb (I), pelvic (II), and pectoral skins (III). The pelvic skin-type AQP protein (green) and urinary bladder-type AQP (red) were expressed in the hindlimb (B and D), pelvic (F and H), and pectoral (J and L) skins in the first reacting cell layer. The greatest number of cells and intensity of labeling were observed in the cytoplasm just beneath the principal cells (arrowheads). Note that differential labeling is visible between the pelvic skin-type AQP and urinary bladder-type AQP. In the absorption test, the immunopositive substances disappeared in the principal cells (C, E, G, I, K, and M). Nuclei are counterstained with DAPI (blue). Scale bar = 10  $\mu$ m. Western blot analysis using anti-AQP-h3 (N, a) detected a major band at  $\sim$ 29 kDa and smeary band with higher molecular masses in the hindlimb skin (lane I), and also weak bands were visible at the identical position in the pelvic (lane II) and pectoral (lane III) skins. In the absorption test (N, b), the immunopositive band disappeared in these regions (lanes I and II). Asterisks indicate nonspecific bands. Similarly, anti-AQP-h2 antibody (O, a) detected a major band at  $\sim$ 29 kDa and smeary bands with higher molecular mass in the hindlimb skin (lane I). Weak bands at the identical position were seen in the pelvic (lane II) and pectoral (lane III) skins. In the absorption test (O, b), the immunopositive band disappeared in these regions. Asterisks indicate nonspecific bands.

10C), and 3 or 4 times in *B. marinus* (Fig. 10D). When hindlimb skin from each species was stimulated with AVT following the  $\text{HgCl}_2$  treatment, the ratio of water flux significantly decreased compared with the AVT stimulation groups (Fig. 10).

#### DISCUSSION

*Importance of the AQP-rich hindlimbs for water absorption by frogs and toads.* Because skin from the hindlimbs was studied separately from the pelvic skin immediately

anterior to the hindlimbs, the present study provides additional details regarding the specialization of ventral skin regions for regulated water absorption by anuran amphibians. Of particular interest, the area-specific rate of AVT-stimulated water flow across isolated skin of the hindlimbs was similarly large for the more mesic and xeric adapted frog and toad species studied. If anything, the response of toad skin was smaller than that of the frog species and tended to be highly variable. This is in contrast with the

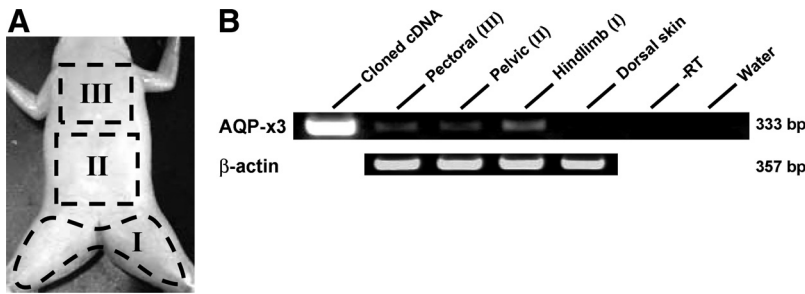


Fig. 5. mRNA expression of the AQP-x3 in the hindlimb, pelvic, and pectoral skins in *Xenopus laevis*. *A*: ventral skin was divided into three regions: hindlimb (*I*), pelvic (*II*), and pectoral skins (*III*). *B*: RT-PCR products obtained using primers as described in Materials and Methods were separated on a 2% agarose gel and stained with ethidium bromide. -RT and water represent the negative control using the hindlimb skin sample without a RT reaction and with water instead of cDNA, respectively.  $\beta$ -actin was used as a positive control. A positive band of AQP-x3 mRNA, the *Xenopus* ventral pelvic type-AQP, was expressed in the hindlimb, pelvic, and pectoral skins.

study of Bentley and Main (4) that used isolated skin from the ventral posterior skin “near the hindlimbs” and found the magnitude of the AVT response to be greatest in *B. marinus* > *H. moori* > *R. pipiens* = *Neobatrachus pelobatoides*. These authors also showed that AVT stimulated water flow across the pectoral skin of *B. marinus* but not the other species. This is consistent with our observations that correlated AVT-stimulated water flow with the presence of an AQP-h2-like water channel in the pectoral region in addition to the pelvic and hindlimb regions of *B. marinus*. For *R. catesbeiana*, AQP-h3-like AQP was observed in the hindlimb and the more anterior pelvic and pectoral regions, while for *R. japonica* and *R. nigromaculata*, it was only observed in the hindlimb. The smaller response to AVT that was observed by Bentley and Main (4) for *Rana* vs. *Bufo*

species could arise from skin obtained near the hindlimb that included a mixture of AQP-rich and AQP-poor regions in contrast with the more extensive distribution of AQPs in the toad skin. Thus, the greater response of *Bufo* vs. *Rana* species, in vivo, could be the result of the relative area of skin that contains AQPs rather than an area-specific response to AVT. As predicted,  $HgCl_2$  inhibited water flux across the hindlimb skin under AVT-stimulation, supporting our assumption that the measured water flux is mediated by mercury-sensitive AQP proteins.

*Possible expression of new-type AQPs in the ventral pelvic skin of Ranid species.* Western blot analysis of the extract of hindlimb skin from *R. japonica*, *R. nigromaculata*, and *R. catesbeiana* revealed a clear band detected at ~29 kDa, which is consistent with the molecular mass

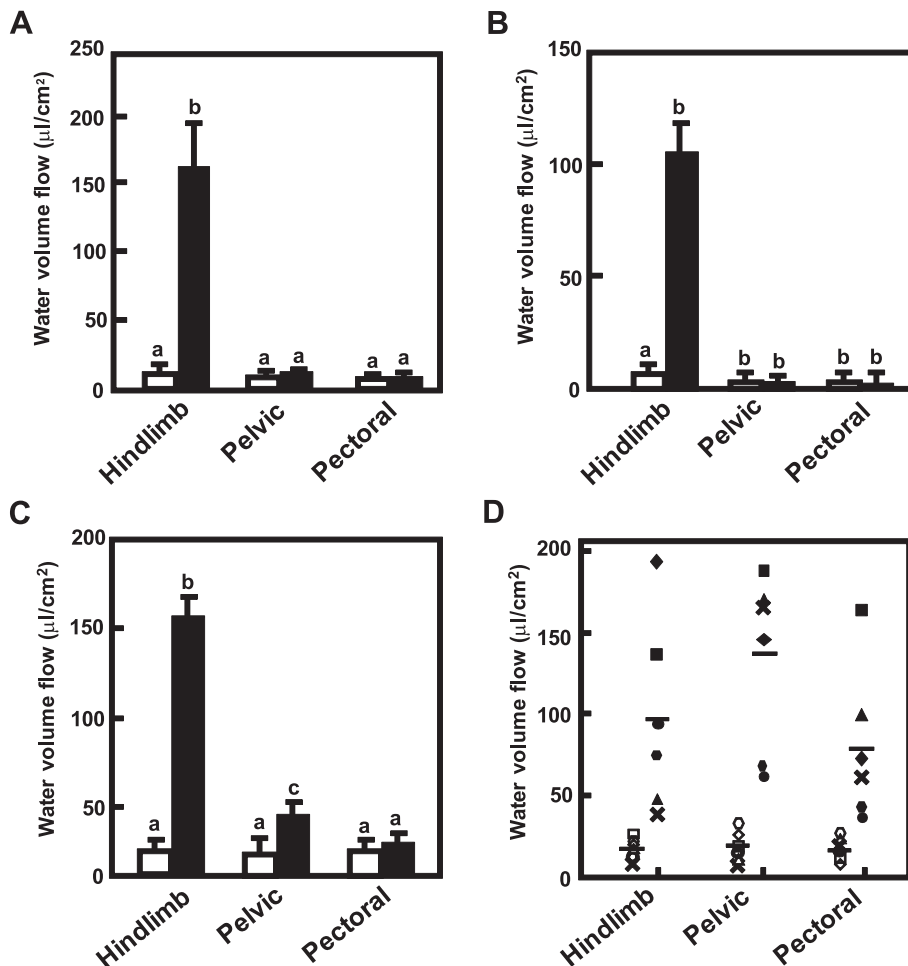


Fig. 6. In vitro water permeability experiment using skin from the hindlimb, pelvic, and pectoral regions evaluated as water flux during 30-min periods before (open bars) and following (solid bars) treatment with  $10^{-8}$  M AVT in the serosal solution. Bars with a different letter (a–c) are significantly different at  $P < 0.05$ . For *R. japonica* (*A*) and *R. nigromaculata* (*B*), AVT treatment significantly increased water permeability in the hindlimb skin, but not in the pelvic or pectoral regions. For *R. catesbeiana* (*C*), the greatest response to arginine vasotocin (AVT) was similarly observed in the hindlimb skin. Smaller responses were detected in the pelvic and pectoral skins. For *B. marinus* (*D*), the response to AVT was different from individual to individual, and even further from tissue to tissue. The same symbol is used to indicate data for each skin region from the same animal.

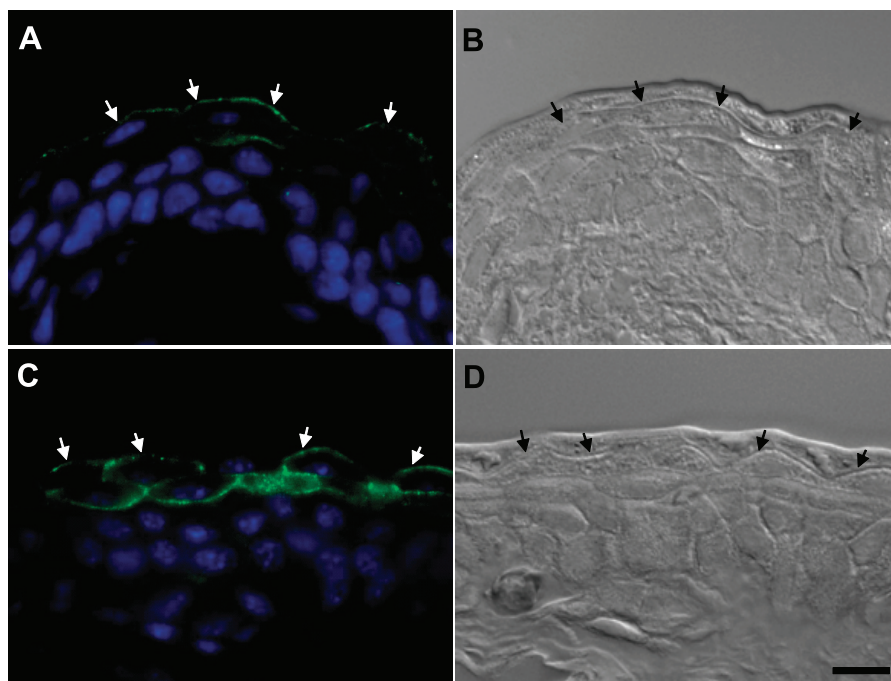


Fig. 7. Immunofluorescence images of the hindlimb skin of *R. japonica* (A, B) and *R. nigromaculata* (C, D) following *in vitro* challenge with  $10^{-8}$  M AVT. In the AVT-treated skins, the label for AQP-h3 (green) was visible in the apical membrane (arrows) of principal cells in the first-reacting cell layers of the hindlimb skin (A, C), while Nomarski images for the same section are shown for reference (B, D). Scale bar = 10  $\mu$ m.

deduced from the amino acid sequences of AQP-h3 isoforms previously cloned for these species (20). It should be noted that AQP-h3 isoforms obtained from extracts of *Xenopus* oocytes injected with cRNA of AQP-h3 isoforms of these species were immunoreactive with the respective antibodies raised for these species. However, the antibody raised against AQP-h3 from *H. japonica* is not immunoreactive with these oocyte extracts (unpublished observation) but does react in the present Western blot analysis of tissue homogenates and immunohistochemically labels hindlimb skins of the three frog species. We have recently cloned a new AQP from the ventral pelvic skin of *R. japonica* that has a higher homology ( $\sim 85\%$ ) with AQP-h3 from *H. japonica*. Extracts of *Xenopus* oocytes injected with cRNA for this AQP-h3-like protein are immunoreactive with the anti-AQP-h3 antibody (unpublished observation). Consequently, the ventral pelvic skin-type AQPs detected by anti-AQP-h3 may be different from those reported previously by Ogushi et al. (20). However, this antibody-specificity was also proven by the absorption test in the present immunohistochemistry and Western blot analyses.

*Physiological and behavioral variables that can affect water absorption.* Because our experiments were conducted during the normal summer activity period on freshly collected animals that were kept with water available *ad libitum*, it seems unlikely that seasonal variability was a factor in the responses of the different species to AVT. It should be noted that Bentley and Main (4) did not report on the seasons during which their study was conducted. Seasonality in the stimulation of water absorption by AVT has been reported in spadefoot toads, *Scaphiopus couchi*, which remain dormant in burrows during much of the year and only respond to AVT during the brief period of emergence during summer rainfall in the southwestern United States (15).

The highly variable values for area-specific water flux across isolated *B. marinus* skin could result from a greater

dependence on vascular perfusion relative to the thinner frog skin. Christensen (9) found that AVT stimulation of water flux across isolated skin from *B. bufo* required the cutaneous vasculature to be perfused with a Ringer solution. The tissue electrolyte content was diluted in nonperfused skin, indicating the circulation removed water as it was absorbed to prevent diminution of the osmotic gradient across the epidermis. Water absorption by anurans occurs in conjunction with a behavior, termed the water absorption response (16, 26), during which the skin is pressed to a moist surface and there is a large increase in blood flow to the absorbing area of the seat patch (33, 34), in conjunction with the insertion of AQPs into the apical membranes of the FRC layer of the skin (27). A better understanding of adaptations for semiterrestrial vs. semiaquatic species will require an understanding of all three parameters from a physiological and phylogenetic perspective.

*Phylogenetic significance on the presence of AQPs of ventral pelvic skin.* Both AQP-h2 and AQP-h3 isoforms are anuran specific AQPs that are structurally distinct from mammalian AQP2 but similarly become inserted into the apical membrane of epithelial cells by antidiuretic hormone stimulation (27). The species differences in the expression and localization of AQP-h2- and AQP-h3- reactive AQPs in the skin raise interesting hypotheses in the context of recent phylogenetic analyses of anuran taxa. On the basis of analysis of morphological and molecular data, Frost et al. (12) suggested that the radiation of anuran families giving rise to modern species occurred when Pangea was breaking up into what would become the current continental land masses, during the Jurassic and Cretaceous periods. The largest superfamilies of extant anurans are the Hyloidea that includes modern Hylid and Bufonid species, among others, and the Ranoidea that includes Ranid species, among others (12, 14, 25). Both *Hyla* and *Bufo* species examined to date have more specialized "seat patch" regions of skin and express AQP-h2-like proteins in the skin and bladder,

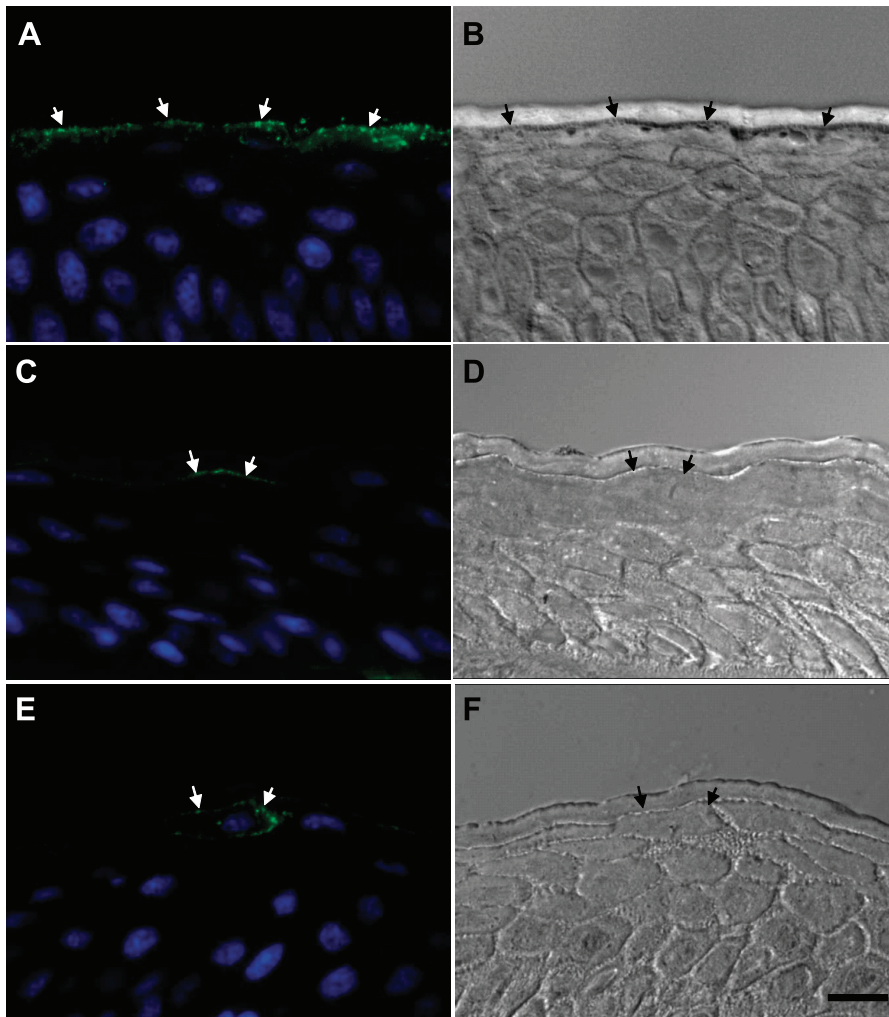


Fig. 8. Immunofluorescence images of the ventral skin of *R. catesbeiana* following in vitro challenge with  $10^{-8}$  M AVT. In the AVT-treated skins, label for AQP-h3 (green) is visible in the apical membrane (arrows) of principal cells in the first-reacting cell layers of the hindlimb skin (A, B). Similar results were obtained in the pelvic (C, D) and pectoral (E, F) skins, although labeled principle cells were fewer in number. Scale bar = 10  $\mu$ m.

indicating this to be an apomorphic character. Further experiments are needed to compare the distribution of this trait and determine its synapomorphic distribution in other families of the Hyloidea.

AQP-h3 has been found in the ventral skin of Bufonid, Hylid, and Ranid species (20, 27), suggesting this pattern of expression is a more pleisiomorphic characteristic. As noted above, we observed AQP-h3 immunoreactivity to be present in the pelvic, as well as hindlimb, skin of *R. catesbeiana*, while it was only present in the hindlimbs of *R. japonica* and *R. nigromaculata*. Recent phylogenetic studies (12) have also noted differences between Ranid species to the point that many taxonomists have reclassified *R. catesbeiana* as *Lithobates catesbeiana*. The North American leopard frog, *Rana pipiens* has similarly been reclassified in the genus *Lithobates* and, like *R. catesbeiana*, the water permeability of its pelvic skin was observed to be modestly stimulated by AVT (4). So-called “old-world” Ranid species, including *R. japonica* and *R. nigromaculata* remain in the genus *Rana*. As with the tissue distribution of AQP-h2-like AQPs, future studies are needed to better determine whether the spatial localization of AQP-h3-like AQPs corresponds with recent advances in phylogenetic analysis of species that have historically been classified as terrestrial, arboreal, and semiaquatic.

*The expression of two AVT-stimulated AQPs in the skin of Bufo and Hyla species.* An AQP-h2 homolog has been detected in the urinary bladder of all species examined but only in the skin of *Hyla* and *Bufo* species (Table 1). In contrast, mRNA encoding an AQP-h3 homolog has been identified in the skin but not the urinary bladder of all species examined (20, 28). Molecular diversity of vasotocin-dependent AQPs closely associated with water adaptation strategy in anuran amphibians. (29). Thus, anurans possess both AQP-h2- and AQP-h3-like AQPs, which respond to AVT, like mammalian AQP2, but are classified into an anuran-specific type, AQP<sub>a2</sub> by phylogenetic analyses (27, 28). For *Xenopus tropicalis*, whose genome data are available in the Ensembl genome browser (<http://www.ensembl.org/index.html>), two types of AQP<sub>a2</sub> genes, i.e., AQP-x2 (ENSXETG00000024581), and AQP-x3 (ENSXETG00000013389), are sited with AQP5 between *FAIM2* (Fas apoptotic inhibitory molecules 2) and *RACGAP1* (Rac GT-Pase-activating protein 1), as are the human genes for AQP2, AQP5, and AQP6 on chromosome 12. On the basis of these findings and the close examination of AQPs in the genome of fishes (medaka and pufferfish), it is likely that h2- and h3-like AQP<sub>a2</sub> genes had been generated by local gene duplication of AQP2 in the amphibian lineage to anurans (28). For contemporary anurans, the upstream regions of these AQP<sub>a2</sub> genes seem to be differentiated so that h2-like AQP<sub>a2</sub>

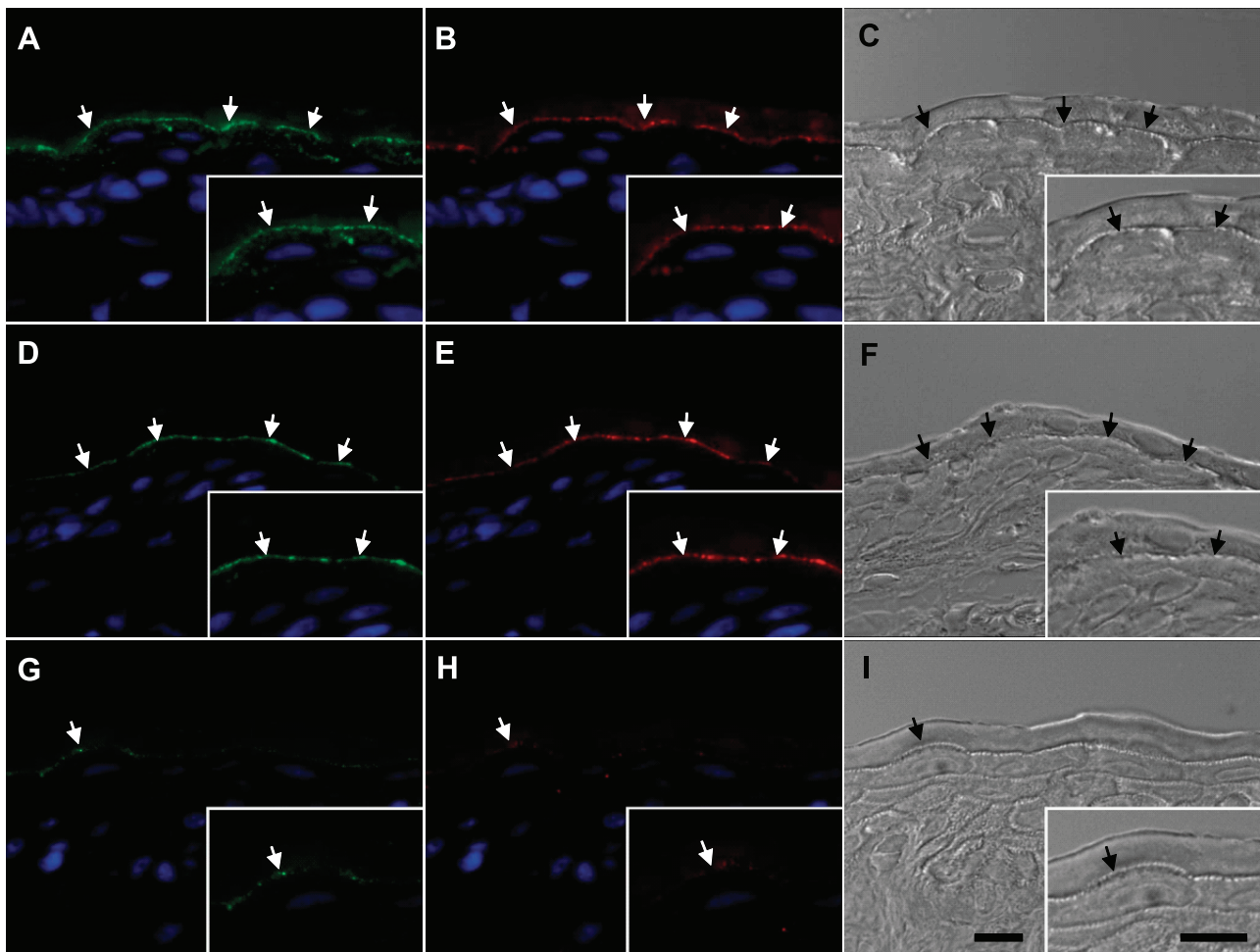


Fig. 9. Immunofluorescence images of the ventral skin of *B. marinus* following in vitro challenge with  $10^{-8}$  M AVT. The label for AQP-h3 (green) and AQP-h2 (red) is visible in the apical membrane (arrows) of principal cells in the first-reacting cell layers of the hindlimb skin (A, B). Similar results were obtained in the pelvic (D, E) and pectoral (G, H) skin, to those in the hindlimb skin, although fewer positive principle cells were labeled. The corresponding Nomarski images (C, F, and I) are to A–B, D–E, and G–H, respectively. The box in each figure is the enlarged image. Nuclei are counterstained with DAPI (blue). Scale bar = 10  $\mu$ m.

basically occurs in the urinary bladder, whereas h3-like AQP $\alpha$ 2 is expressed in the ventral skin. In *Bufo* and *Hyla* species, the upstream region of h2-like AQP $\alpha$ 2 gene is considered to have undergone a further change to express this gene in the ventral skin, as well as in the urinary bladder, which might give the terrestrial species an advantage with respect to cutaneous water absorption and thereby in adapting to drier environments.

*A unique AQP in aquatic Xenopus.* The purely aquatic species in the family, Pipidae, are believed to have diverged from other anurans as far back as the Permian period (12). *X. laevis* is a commonly used species for a variety of molecular and developmental studies but lacks a hydroosmotic response to AVT (3, 4, 36). Nonetheless, we have identified mRNA of AQP-x3 in the pelvic skin of *X. laevis* that is homologous to AQP-h3, but contains an extra C-terminal tail, consisting of 33 nucleotides within the coding region, which appears to attenuate translation (22). Despite the lack of functional expression of the protein, we have shown mRNA for AQP-x3 to be present in all three regions of the ventral skin. In their native habitat, ponds may dry up and leave the animals dependent on

substrate moisture (32). Under these conditions, complete processing of the mRNA and expression of AQP-x3 could be advantageous, but we are unaware of data to support this possibility.

*Regulation of AQP expression by AVT and its related peptides.* In the present study, we found that hydrin 1 and hydrin 2 stimulated the water permeability of the hindlimb skin of *Bufo* and *Rana* species at a level equivalent to that of AVT. The  $K_m$  for cAMP production by tree frog  $V_2$ -type AVT receptor expressed by transfected CHO-K1 cells was 3.6, 8.6, and 13.5 nM for AVT, hydrin 1, and hydrin 2, respectively (18), suggesting they may share a common receptor. Both peptides are generated from a down-regulation in posttranslational processing, i.e., hydrin 1 by a decrease in carboxypeptidase E activity and hydrin 2 by a reduction in the activity of the  $\alpha$ -amidating enzymatic system. Of interest, *X. laevis* secretes hydrin 1, as well as AVT but shows no hydroosmotic response of skin to either. However, AVT and hydrin 1 both stimulate water reabsorption from the urinary bladder and may be involved in the water balance in *X. laevis* during aestivation (24).

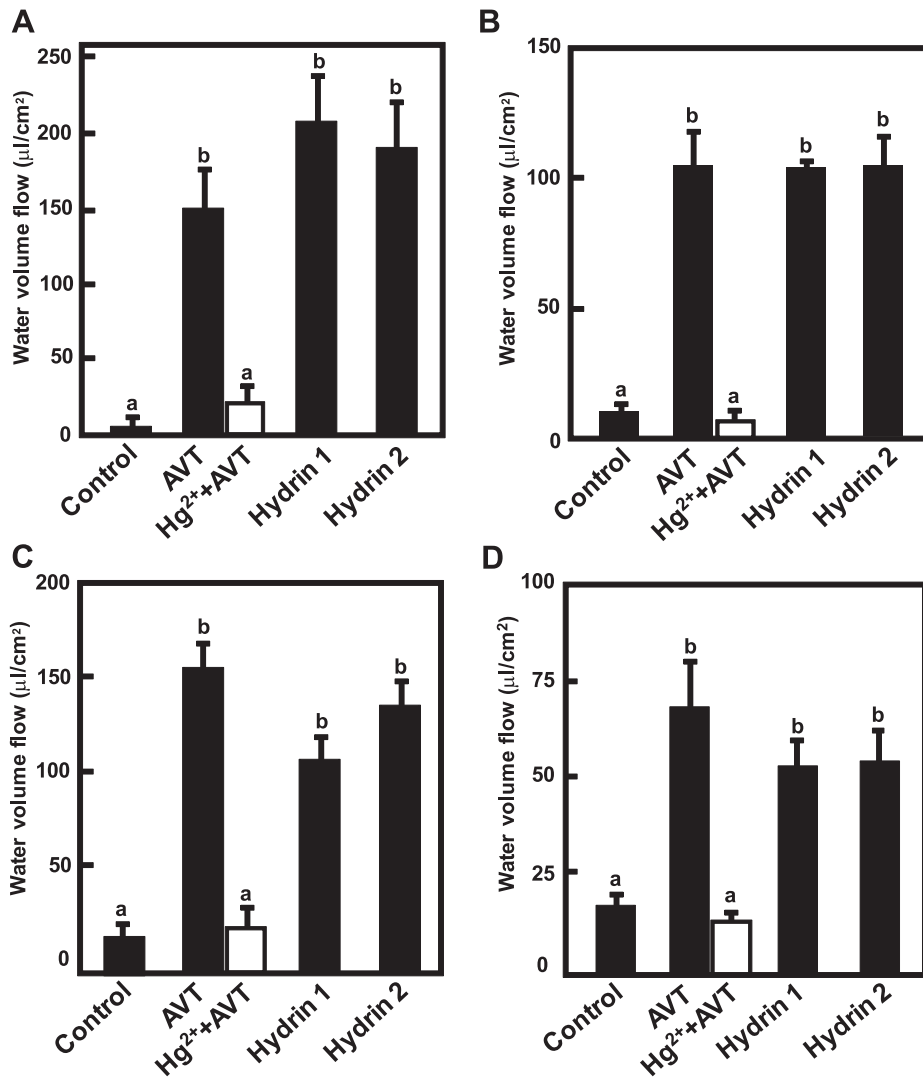


Fig. 10. AVT, hydrin 1, hydrin 2, and HgCl<sub>2</sub> stimulated the water permeability across hindlimb skin of *R. japonica* (A), *R. nigromaculata* (B), *R. catesbeiana* (C), and *B. marinus* (D). The response to the three peptides was not significantly different within a species, but the response of *B. marinus* was smaller than that of the *Rana* species. HgCl<sub>2</sub> inhibited water flux to the control levels even under stimulation of AVT (Hg<sup>2+</sup> + AVT). Scale bars with a different letter (a, b) are significantly different at  $P < 0.05$ .

### Perspectives and Significance

Anuran amphibians have two AQP isoforms that are stimulated by AVT to increase water absorption across the skin and reabsorption from the urinary bladder. Suzuki and Tanaka (28) suggested the two isoforms are derived from gene duplication of AQP2 in an ancestral amphibian and are homologs of AQP-h2 and AQP-h3 that were first characterized in *H. japonica*. Amniotes, including mammals, are thought to have evolved from a primitive amphibian ancestor in the carboniferous (8) and retain AQP2 as a single isoform regulated by antidiuretic hormone, while amphibian evolution has proceeded independently. Given the importance of regulated water permeability in amphibian skin and bladder, the two isoforms have retained the same function in the course of evolution.

Within the limited number of species examined, anurans in the superfamily Hyloidea express both isoforms in the ventral skin and have a specialized seat patch region that is also highly vascularized. Anurans in the superfamily Ranidae lack specialization in the pelvic region and express only AQP-h3, primarily in the ventral surface of the hindlimbs. The aquatic frog, *X. laevis* transcribes mRNA for homologs

of both isoforms but a C-terminal sequence prevents translation. However, all species examined to date express AQP-h2-like AQPs in the urinary bladder. Future studies are needed to examine species differences in the functional expression of AQP-h2 and AQP-h3 to characterize phylogenetic relationships associated with water balance adaptations among anuran families.

### ACKNOWLEDGMENTS

We thank Ms. Istuha Katsube of Naha Nature Conservation Office Ishigaki Ranger Office for her kind help collecting animals.

### GRANTS

This work was supported in part by grants-in-aid for scientific research (19370024; 20570055) from the Ministry of Education, Culture, Sports, Science and Technology of Japan, by a grant-in-aid from the Japan Society for the Promotion of Science (21.3448) to Y. Ogushi, and by a SUNBOR grant from Suntory Institute for Bioorganic Research to S. Tanaka and M. Suzuki.

### DISCLOSURES

No conflicts of interest, financial or otherwise, are declared by the authors.

## REFERENCES

1. **Agre P.** The aquaporin water channels. *Proc Am Thorac Soc* 3: 5–13, 2006.
2. **Akabane G, Ogushi Y, Hasegawa T, Suzuki M, Tanaka S.** Gene cloning and expression of an aquaporin (AQP-h3BL) in the basolateral membrane of water-permeable epithelial cells in osmoregulatory organs of the tree frog. *Am J Physiol Regul Integr Comp Physiol* 292: R2340–R2351, 2007.
3. **Bentley PJ.** The Amphibia. In: *Endocrines and Osmoregulation. A Comparative Account in Vertebrates*, edited by Bentley PJ, vol. 39. New York: Springer, 2002, p. 155–186.
4. **Bentley PJ, Main AR.** Zonal differences in permeability of the skin of some anuran Amphibia. *Am J Physiol* 223: 361–363, 1972.
5. **Bentley PJ, Yorio T.** Do frogs drink? *J Exp Biol* 79: 41–46, 1979.
6. **Brown D, Grosso A, DeSousa RC.** Correlation between water flow and intramembrane particle aggregates in toad epidermis. *Am J Physiol Cell Physiol* 245: C334–C342, 1983.
7. **Brown D, Ilic V.** Freeze fracture differences in plasma membranes of the stratum corneum and replacement layer cells of amphibian epidermis. *J Ultrastruct Res* 67: 55–64, 1979.
8. **Carroll RL.** The origin and early radiation of terrestrial vertebrates. *J Paleontol* 75: 1202–1213, 2001.
9. **Christensen CU.** Adaptations in the water economy of some anuran amphibia. *Comp Biochem Physiol A Comp Physiol* 47: 1035–1049, 1974.
10. **Dole JW.** The role of substrate moisture and dew in the water economy of leopard frogs. *Rana pipiens*. *Copeia* 1967: 141–149, 1967.
11. **Farquhar MG, Palade GE.** Cell junctions in amphibian skin. *J Cell Biol* 26: 263–291, 1965.
12. **Frost D, Grant T, Faivovich J, Bain RH, Haas A, Haddad HFE, De Sa RO, Channing A, Wilkinson M, Donnellan SC, Raxworthy CJ, Campbell, JA, Blotto BL, Moler P, Drewes RC, Nussbaum RA, Lynch JD, Green DM, Wheeler WC.** The amphibian tree of life. *Bull Am Mus Nat Hist Series* 297: p. 1–370, 2006.
13. **Hasegawa T, Tani H, Suzuki M, Tanaka S.** Regulation of water absorption in the frog skins by 2 vasotocin-dependent water-channel aquaporins, AQP-h2 and AQP-h3. *Endocrinology* 144: 4087–4096, 2003.
14. **Hillman SS, Withers PC, Drewes RC, Hillyard SD.** Ecological and environmental physiology of amphibians. New York: Oxford University Press, 2009, p. 1–469.
15. **Hillyard SD.** Variation in the effects of antidiuretic hormone on the isolated skin of the toad, *Scaphiopus couchi*. *J Exp Zool* 195: 199–206, 1976.
16. **Hillyard SD, Hoff KS, Propper C.** The water absorption response: a behavioral assay for physiological processes in terrestrial amphibians. *Physiol Zool* 71: 127–138, 1998.
17. **Ishibashi K, Kuwahara M, Sasaki S.** Molecular biology of aquaporins. *Rev Physiol Biochem Pharmacol* 141: 1–32, 2000.
18. **Kohno S, Kamishima Y, Iguchi T.** Molecular cloning of an anuran V(2) type [Arg(8)] vasotocin receptor and mesotocin receptor: functional characterization and tissue expression in the Japanese tree frog (*Hyla japonica*). *Gen Comp Endocrinol* 132: 485–498, 2003.
19. **Michel G, Ouedraogo Y, Chauvet J, Katz U, Acher R.** Differential processing of provasotocin: relative increase of hydrin 2 (vasotocinyl-Gly) in amphibians able to adapt to an arid environment. *Neuropeptides* 25: 139–143, 1993.
20. **Ogushi Y, Akabane G, Hasegawa T, Mochida H, Matsuda M, Suzuki M, Tanaka S.** Water adaptation strategy in anuran amphibians: molecular diversity of aquaporin. *Endocrinology* 151: 165–173, 2010.
21. **Ogushi Y, Kitagawa D, Hasegawa T, Suzuki M, Tanaka S.** Correlation between aquaporin and water permeability in response to vasotocin, hydrin, and  $\beta$ -adrenergic effectors in the pelvic skin of the tree frog, *Hyla japonica*. *J Exp Biol* 213: 288–294, 2010.
22. **Ogushi Y, Mochida H, Nakakura T, Suzuki M, Tanaka S.** Immunocytochemical and phylogenetic analyses of an arginine vasotocin-dependent aquaporin, AQP-h2K, specifically expressed in the kidney of the tree frog, *Hyla japonica*. *Endocrinology* 148: 5891–5901, 2007.
23. **Preston GM, Carroll TP, Guggino WB, Agre P.** Appearance of water channels in *Xenopus* oocytes expressing red cell CHIP28 protein. *Science* 256: 385–387, 1992.
24. **Rouille Y, Michel G, Chauvet MT, Chauvet J, Acher R.** Hydrins, hydrosomatic neurohypophysial peptides: osmoregulatory adaptation in amphibians through vasotocin precursor processing. *Proc Natl Acad Sci USA* 86: 5272–5275, 1989.
25. **San Mauro D, Vences M, Alcobendas M, Zardoya R, Meyer A.** Initial diversification of living amphibians predated the break-up of Pangaea. *Am Nat* 165: 590–599, 2006.
26. **Stille WT.** The water absorption response of an anuran. *Copeia* 1958: 217–218, 1957.
27. **Suzuki M, Hasegawa T, Ogushi Y, Tanaka S.** Amphibian aquaporins and adaptation to terrestrial environments: a review. *Comp Biochem Physiol A* 148: 72–81, 2007.
28. **Suzuki M, Tanaka S.** Molecular and cellular regulation of water homeostasis in anuran amphibians by aquaporins. *Comp Biochem Physiol Part A* 153: 231–241, 2009.
29. **Suzuki M, Tanaka S.** Molecular diversity of vasotocin-dependent aquaporin closely associated with water adaptation strategy in anuran amphibians. *J Neuroendocrinol* 22: 407–412, 2010.
30. **Takata K, Matsuzaki T, Tajika Y.** Aquaporins: water channel proteins of the cell membrane. *Prog Histochem Cytochem* 39: 1–83, 2004.
31. **Tani H, Hasegawa T, Hirakawa N, Suzuki M, Tanaka S.** Molecular and cellular characterization of a water channel protein, AQP-h3, specifically expressed in the frog ventral skin. *J Membrane Biol* 188: 43–53, 2002.
32. **Tinsley RC, Loumont C, Kobel HR.** Geographical distribution and ecology. In: *The Biology of Xenopus*, edited by Tinsley RC and Kobel HR, Oxford: Clarendon, 1996, p. 35–59.
33. **Viborg AL, Hillyard SD.** Cutaneous blood flow and water absorption by dehydrated toads. *Physiol Biochem Zool* 78: 394–404, 2005.
34. **Viborg AL, Rosenkilde P.** Water potential receptors in the skin regulate blood perfusion in the ventral pelvic patch of toads. *Physiol Biochem Zool* 77: 39–49, 2004.
35. **Voute CL, Ussing HH.** Some morphological aspects of active sodium transport. The epithelium of the frog skin. *J Cell Biol* 36: 625–638, 1968.
36. **Yorio T, Bentley PJ.** The permeability of the skin of the aquatic anuran *Xenopus laevis* (Pipidae). *J Exp Biol* 72: 285–289, 1978.
37. **Zimmerman SL, Frisbie J, Goldstein DL, West J, Rivera K, Krane CM.** Excretion and conservation of glycerol, and expression of aquaporins and glyceroporins, during cold acclimation in Cope's gray treefrog, *Hyla chrysocelis*. *Am J Physiol Regul Integr Comp Physiol* 292: R544–R555, 2007.